CrystEngComm

Discrimination of two crystal forms of $DyBa_2Cu_3O_{7-\delta}$ superconductor: tetragonal and orthorhombic forms having very close lengths of axis

Journal:	*CrystEngComm*
Manuscript ID	CE-ART-03-2022-000306.R1
Article Type:	Paper
Date Submitted by the Author:	03-Apr-2022
Complete List of Authors:	Kimura, Fumiko; Kyoto University of Advanced Science, Faculty of Engineering Adachi, Shintaro; Kyoto University of Advanced Science, Nagamori Institute of Actuators Horii, Shigeru; Kyoto University Graduate School of Energy Science Kimura, Tsunehisa; Fukui University of Technology, Department of Applied Science and Engineering

ARTICLE

Discrimination of two crystal forms of $DyBa_2Cu_3O_{7-\delta}$ superconductor: tetragonal and orthorhombic forms having very close lengths of axis

Received 00th January 20xx,
Accepted 00th January 20xx

DOI: 10.1039/x0xx00000x

Fumiko Kimura,*[a] Shintaro Adachi,[b] Shigeru Horii,[a] and Tsunehisa Kimura [c]

The oxygen content in $DyBa_2Cu_3O_{7-\delta}$ ($0 \leq \delta \leq 1$) greatly affects superconductivity. When the oxygen content is high, the crystal takes an orthorhombic form and exhibits superconductivity, while it takes a tetragonal form, which is not superconductive, when the oxygen content is low. It is difficult to discriminate between these two forms using powder X-ray diffraction (XRD), especially when the oxygen content is around the transition region between orthorhombic and tetragonal forms; around the transition region, the orthorhombic *a* and *b* axes are close to each other, and the tetragonal *a* axis is close to the orthorhombic *a* axis. Such cases may occur not only in the present compound but also in other compounds. In this study, $DyBa_2Cu_3O_{7-\delta}$ samples were prepared near the transition conditions. The powder sample was suspended in a liquid medium and subjected to a magnetic field with or without a sample rotation, and in situ XRD measurements were performed to obtain two different XRD patterns. The analysis of these patterns allowed us to identify a mixture of two crystal forms. The mixing ratio depended on the preparation condition.

Introduction

The superconducting properties of high-T_c $REBa_2Cu_3O_{7-\delta}$ (RE: rare earth; $\mathbf{0 \leq \delta \leq 1}$) superconductors are highly sensitive to oxygen content.[1] Since the crystal structure strongly depends on the oxygen content, characterization of the sample via XRD is very useful[1-3]. In some cases, the prepared sample can be a mixture of crystals with slightly different lengths of the *a* and *b* axes, complicating the characterization of the crystal structure. Depending on the preparation conditions, a mixture of orthorhombic and tetragonal forms may occur, especially when the δ value is in the transition region between these two crystal forms. Under these circumstances, powder XRD has limitations in characterizing the sample.

Since the $REBa_2Cu_3O_{7-\delta}$ crystal is paramagnetic, its magnetic anisotropy[4, 5] is high compared to diamagnetic crystals. Its microcrystals are highly aligned under relatively weak magnetic fields, such as those created by neodymium magnets. It is known that the tetragonal and orthorhombic forms can be easily distinguished in 2D (two-dimensional) XRD patterns obtained from magnetic orientation of the microcrystals in the suspension[6]. In this study, this technique is used to analyze the sample.

In this report, $DyBa_2Cu_3O_{7-\delta}$ crystals prepared under several different experimental conditions were characterized by analyzing the two 2D XRD patterns obtained via magnetic orientation. The orthorhombic and tetragonal forms were clearly distinguished, which was not possible with only a one-dimensional powder XRD pattern. It was found that the sample obtained via heat treatment is very sensitive to the experimental conditions: even under supposedly the same experimental condition, the crystal form was different.

Experimental

Preparation of polycrystalline Dy123 powder

The starting materials, Dy_2O_3, $BaCO_3$, and CuO, were weighed at a cation ratio of 1:2:3 and ground thoroughly with ethanol. The mixed powder was calcined at 880°C, followed by grinding at room temperature; then the process was repeated at calcination temperatures of 900 and 920°C. The obtained specimen was then pelletized and sintered at 950°C for 24 h to obtain a polycrystalline sample.

Preparation of fully oxidized Dy123 ($\delta \sim 0$)

The obtained polycrystalline sample was annealed in two steps: initially under a 100% O_2 gas flow at 450˚C for 40 h, and then under a 100% O_2 gas flow at 300˚C for 40 h. After the heater was turned off, the samples were cooled to room temperature with the 100% O_2 gas flow. The prepared sample is denoted as 300#1.

Preparation of oxygen-reduced Dy123 powder

The obtained polycrystalline sample was annealed at 650, 700, or 800 ˚C for more than 100 h by flowing 0.1% O_2 gas (a mixture of 99.9% Ar and 0.1% O_2) at a flow rate of 100 mL/min. During the quenching process, the 0.1% O_2 gas was run until the sample

[a] *Department of Engineering, Kyoto University of Advanced Science, Yamanouchi-Gotandacho, Ukyo-ku, Kyoto 615-8577, Japan.*
[b] *Nagamori Institute of Actuators, Kyoto University of Advanced Science, Yamanouchi-Gotandacho, Ukyo-ku, Kyoto 615-8577, Japan.*
[c] *Department of Applied Science and Engineering, Fukui University of Technology, 3-6-1 Gakuen, Fukui 910-8505, Japan*
† Footnotes relating to the title and/or authors should appear here.
Electronic Supplementary Information (ESI) available: [details of any supplementary information available should be included here]. See DOI: 10.1039/x0xx00000x

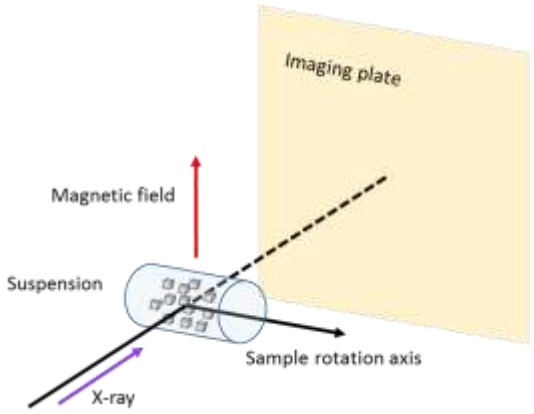

Figure 1 In-situ 2D XRD measurement. The sample suspension is rotated while XRD measurement.

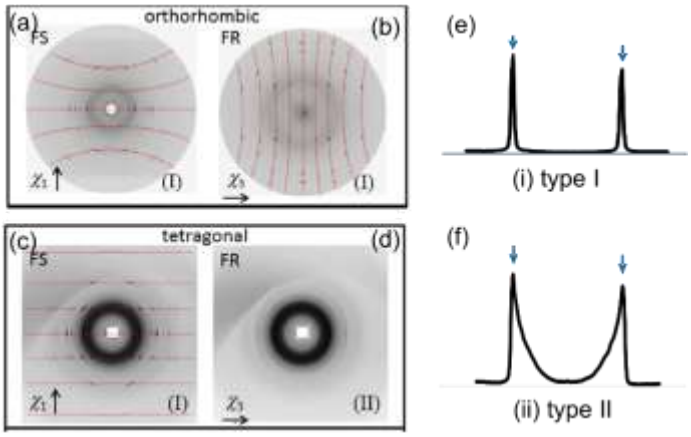

Figure 2 Typical 2D XRD patterns of the orthorhombic form (L-alanine (a), (b)) and tetragonal form (urea (c), (d)) measured without ((a), (c)) and with ((b), (d)) sample rotation in a magnetic field. The patterns in (a), (b), and (c) show sharp peaks on the azimuthal plot of a (hkl) plane, as shown in (e). The pattern in (d) shows a unique azimuthal plot of a (hkl) plane, as shown in (f). The measurements with sample rotation make it possible to discriminate between the orthorhombic and tetragonal forms. This is possible when $\chi 1 > \chi 2 = \chi 3$, which is the case in the present study. See reference 6 for details. "Reprinted with permission from { Matsumoto, K.; Kimura, F.; Song, G.; Yamane, S.; Kikuchi, H.; Tanaka, T.; Higuchi, S.; Kitamura, N.; Kimura, T., Crystal System Determination from X-ray Diffraction of Magnetically Oriented Microcrystal Suspensions. Crystal Growth & Design 2014, 14 (12), 6486-6491}. Copyright 2014 American Chemical

reached room temperature to prevent oxidization of the sample. The prepared samples are denoted as 650#1, 700#1, 700#2, 800#1, and 800#2 ("#2" indicates that a second sample was prepared in addition to the first one, "#1," under the same conditions).

Pulverization process

The fully oxidized and oxygen-reduced polycrystalline pellets were crushed in an agate mortar for usage.

Preparation of suspensions

We dispersed 0.02–0.04 g of Dy123 microcrystalline powder in 0.2–0.4 g of a standard liquid for calibrating viscometers (JS14000, Nippon Grease Co. Ltd., Tokyo, Japan; viscosity: 12 Pa s at 293℃) to prepare ca. 10 wt% microcrystalline suspensions.

Powder XRD measurement

Powder X-ray diffraction measurements were performed at room temperature using the continuous scanning mode of an Ultima IV diffractometer (CuKα radiation; Rigaku Corporation, Japan) with a scanning rate of 3°/min and a step size of 0.02°.

Data processing I

The unit cell dimensions of samples were determined from the *d* spacing calculated via a least-squares method using Cellcalc[7], assuming that the structures are orthorhombic or tetragonal.[8]

Magnetic alignment

About 0.02 mL of each suspension was placed in a glass tube. The tube was mounted on a sample-rotating unit and subjected to a vertical static magnetic field generated by a pair of permanent magnets (Fig. 1; the magnetic field is 1 T). A rotating magnetic field was obtained via uniform sample rotation of 180 rpm in a static magnetic field.

Two 2D XRD measurements

In situ XRD measurements were performed at room temperature using MoKα radiation for the measurements in static and rotating magnetic fields, with a two-dimensional detector (R-AXIS RAPID II, Rigaku Corporation). The suspension-to-detector distance was 14.7 mm.

Data processing II

Using 2D data processing software (2DP, Rigaku Corporation), the diffraction intensities were integrated at 2ϑ = ca. 14.85° for the study of orientation dynamics under the static magnetic field and the rotating magnetic field with a width of 1.5° in 0.5° steps to obtain the azimuthal β profile.

Figure 1 shows an experimental setup of in situ X-ray diffraction measurement. In situ XRD measurements were performed with and without sample rotation to collect two 2D XRD patterns. The rotation speed of the sample was 180 rpm. This speed was high enough for the microcrystals to rotate in the viscous suspending medium.[9] A set of recorded 2D patterns (with and without rotation) enables us to distinguish the crystal form of the samples.[6]

Results and discussion

Results and discussion

Figure 2 shows a general example of how the crystal form is determined, using two 2D XRD patterns obtained with and without sample rotation in a magnetic field with the setting shown in Fig. 1.[6] For the orthorhombic form, the magnetic χ_1, χ_2, and χ_3 axes are parallel to the crystallographic *a*, *b*, and *c* axes, respectively. Here, we assume $\chi_1 > \chi_2 > \chi_3 > 0$. The χ_1 and χ_3 axes are referred to as easy and hard magnetization axes, respectively. The χ_1 and χ_3 axes align uniaxially without and with sample rotation, respectively, giving rise to two 2D XRD patterns with layered sharp XRD spots (Fig. 2a, b). The azimuthal β-plot for a given 2θ produces sharp peaks, as shown in Fig. 2e. We call this type of diffraction pattern Type I. On the other hand, in the tetragonal form, one of the magnetic axes, the χ_1 axis, for example, corresponds to the crystallographic major axis, the *c* axis. As a result, the 2D XRD pattern with layered sharp XRD spots appears for the static measurement (Fig. 2c), and a wide arc-shaped XRD pattern symmetric with respect to the meridian appears (Fig. 2d), whose azimuthal plot exhibits a horn-like peak as shown in Fig. 2f. We call this type of XRD Type II.

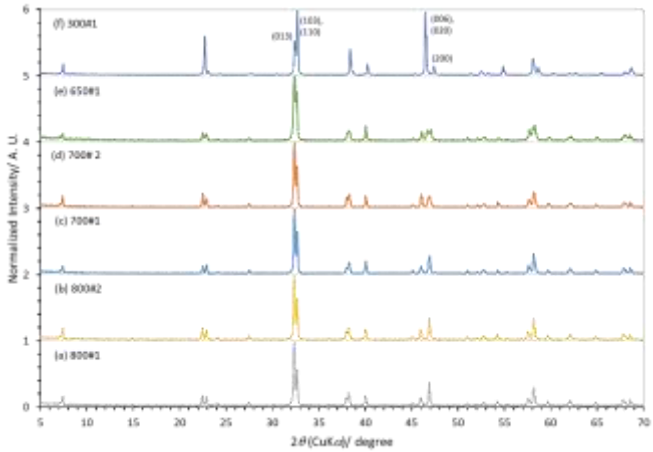

Figure 3 Powder XRD patterns of the samples prepared in this study. The sample is named T#n, where T and n denote the annealing temperature and the sample number, respectively. The oxygen concentration during the annealing was 0.1% except for (f). The oxygen concentration was 100% for 300#1 (f). Note that the X-ray source is CuKα.

The lattice parameters of the orthorhombic Dy123 are a = 3.8931 Å, b = 3.8307 Å, and c = 11.7168 Å.[10] The crystallographic axes correspond to the magnetic χ_1, χ_2, and χ_3 axes, such as $\chi_1 \| c$, $\chi_2 \| a$, and $\chi_3 \| b$.[11-13] The crystallographic axes of the tetragonal form correspond to the magnetic $\chi_1 > \chi_2 = \chi_3$ ($\equiv \chi$) axes, such as $c \| \chi_1$, $a \| \chi$, and $b \| \chi$.

Figure 3 shows the powder XRD patterns for the six samples ((a) 800#1, (b) 800#2, (c) 700#1, (d) 700#2, (e) 650#1, and (f) 300#1). The pattern in (f) is clearly distinguished from the others, but those in (a) to (e) differ only slightly in peak position and intensity. Sample 300#1 was prepared at 300°C, which was a fully oxidized orthorhombic form ($DyBa_2Cu_3O_{7-\delta}$, $\delta \approx 0$), so the peak assignments were possible and included in the figure. The others were annealed between 800°C and 650°C and may be a tetragonal form, a partially oxidized orthorhombic form ($0<\delta<1$), or a mixture of the two forms. If the annealing temperature happened to be close to the orthorhombic-to-tetragonal transition temperature, the peak position of the partially oxidized orthorhombic form will be much closer to that of the tetragonal form, making it difficult to characterize the prepared samples.

Figure 4(I) shows an enlarged view of the region with the highest diffraction intensity. Samples 800#1 (a) and 800#2 (b) are presumed to be rich in tetragonal forms. The peak position

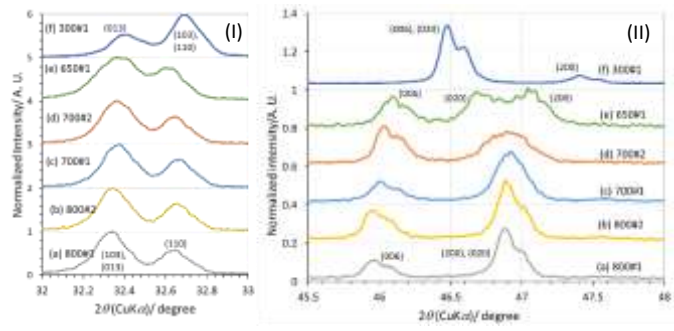

Figure 4 Enlargements of the 2θ region of Fig. 3. (I) 32-33° and (II) 45.5-48°.

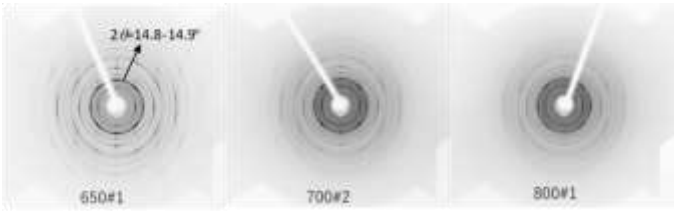

Figure 5 2D XRDs for 650#1, 700#2 and 800#1 obtain with sample rotation. The diffraction at 2θ= 14.8-14.9° (MoKα) assignable to the (013), (103), and (110) planes of the tetragonal and orthorhombic forms are marked.

and intensity change gradually from (a) to (e). Those of 650#1 (e) are clearly different from those of 300#1 (f) (fully oxidized). Samples (a) through (e) may be tetragonal, partially oxidized orthorhombic, or a mixture of both. Figure 4(II) shows an enlarged view of the region around 2θ = 47°. The assignment of the (200), (020), and (006) diffractions for 800#1 (a) (presumed to be tetragonal) and 300#1 (f) is indicated. Note that the shoulders near 2θ = 47° (clearly visible in 800#1 and 800#2) are due to CuKα_2 diffraction. The tetragonal peak for 800#1 broadens with decreasing treatment temperature, and it splits into two peaks in 650#1 that may be assigned to partially oxidized orthorhombic (200) and (020) diffractions. Perhaps the orthorhombic-to-tetragonal transition occurs at around 650–700°. Although 700#1 and 700#2 are samples prepared under the same experimental condition, their peak profiles are clearly different. The poor reproducibility may be attributed to the fact that this temperature is in the transition region. In contrast, the reproducibility for 800#1 and 800#2 is good.

Figure 5 shows the 2D XRDs of samples 650#1, 700#2, and 800#1 measured while the sample suspension was rotating. Under this experimental condition, the orthorhombic b axis ($\| \chi_3$) aligns parallel to the equator, and the ($h0l$) diffractions appear on the meridian. Sample 650#1 clearly exhibits a Type I

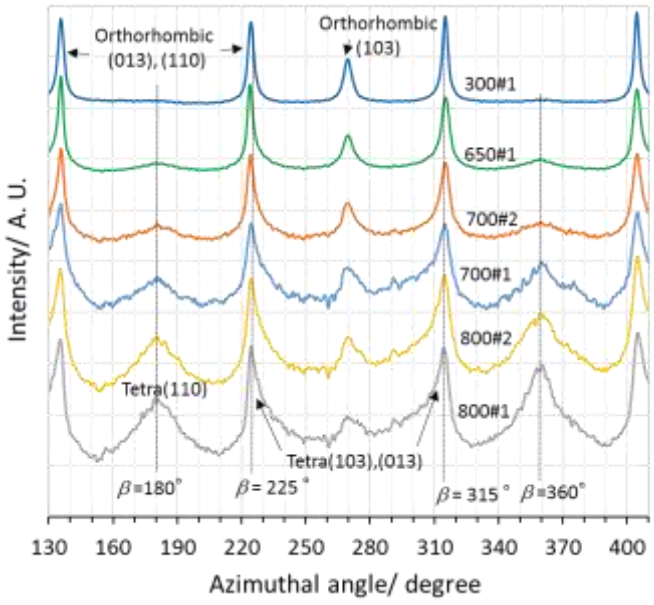

Figure 6 Azimuthal β scans taken for the 2θ range shown in Fig. 4 (I), which includes the (013), (103), and (110) diffraction planes of the tetragonal and orthorhombic forms.

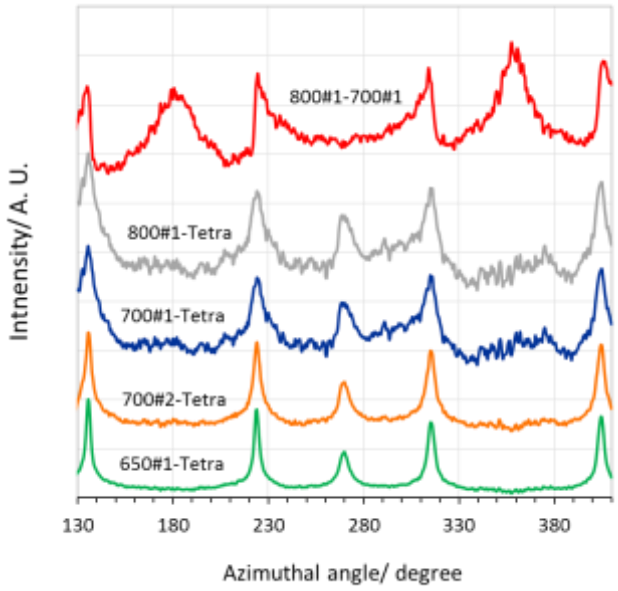

Figure 7 Subtraction XRD patterns to separate pure tetragonal and orthorhombic forms. The subtraction pattern (800#1-700#1) is attributed to the pure tetragonal form denoted as Tetra. Tetra is subtracted from 800#1, 700#1, 700#2, and 650#1 to obtain the diffraction of the pure orthorhombic forms contained in these samples.

pattern, indicating that it is an orthorhombic form. The patterns of 700#2 and 800#1 are regarded as Type II. On the other hand, all six samples obtained under a static magnetic field exhibit Type I patterns (the results are not shown).

For closer examination, an azimuthal β scan was performed for the six samples. Figure 6 shows the azimuthal β scans taken for the 2θ range used in Fig. 4 (I). The diffractions of (103), (013), and (110) appear at 2θ = 32.3–32.7° and 14.8–14.9° with the CuKα and MoKα sources, respectively. The fully oxidized sample 300#1 exhibits the (103) peak in the meridional direction (β =270°) and the (110) and (013) peaks at β =225° and β = 315°. Partially oxidized orthorhombic or tetragonal diffraction spots are also assumed to appear at 2θ = approximately 14.8–14.9°. Two broad peaks on the equator (β =180° and 360°) are the result of merging two pairs of the Type II peaks originating from the tetragonal form. Thus, the intensity of these peaks is a measure of the tetragonal content. A pair of peaks located at β =225° and β = 315° may originate from a mixture of Type II diffraction due to the tetragonal (103) and (013) and Type I diffraction due to the orthorhombic (110) and (013). Samples 650#1 and 700#2 show significantly reduced peak intensity on the equator, indicating that the tetragonal content of these samples is low. Furthermore, a pair of peaks at β =225° and β = 315° are sharp and symmetrical, indicating higher orthorhombic content. Thus, the samples 650#1 and 700#2 are characterized as having low tetragonal content and high orthorhombic content. In contrast, samples 800#1, 800#2, and 700#1 exhibit high intensity on the equator, indicating high tetragonal content. Low content of the orthorhombic form is indicated by an obscured meridional peak and the asymmetric shape of the peaks at β =225° and β = 315°. To conclude, the five samples are mixtures of the tetragonal and orthorhombic forms, where 800#1, 800#2, and 700#1 are rich in tetragonal and 700#2 and

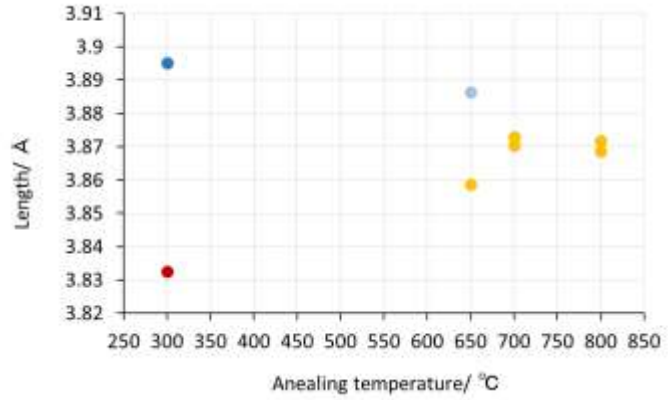

Figure 8 The length of the *a* and *b* axes of $DyBa_2Cu_3O_{7-\delta}$ as a function of the annealing temperature obtained by analyzing the powder XRD profiles in Fig. 3. ●: *a* axis under flowing 0.1% O_2 gas; ●: *b* axis under flowing 0.1% O_2 gas; ●: *a* axis under flowing 100% O_2 gas; ●: *b* axis under flowing 100% O_2 gas.

650#1 are rich in orthorhombic forms. The above interpretation is supported by examining the subtraction profile.

The crystal orderliness of the orthorhombic form in each mixture was examined by using subtraction profiles. In Fig. 7, the subtraction of 700#1 from 800#1 is performed so that the peaks on the meridian (β =270°), attributed to the orthorhombic form, are completely removed. The resulting profile shows horn-like peaks at β = 225 and 315° and broad peaks on the equator. This typical Type II profile is attributed to the tetragonal form contained in 700#1 and 800#1. Figure 7 also shows the subtraction profile of a pure tetragonal form (800#1-700#1) from 800#1, 700#1, 700#2, and 650#1 so that the broad peaks on the equator, attributed to the pure tetragonal form, are completely removed. The obtained profiles show sharp peaks located at β = 225, 270, and 315°. These peaks are attributed to a Type I pattern originating from the orthorhombic forms contained in 800#1, 700#1, 700#2, and 650#1. The sharpness of the orthorhombic peaks in these profiles are slightly different. The peaks in the profiles for 800#1 and 700#1 are less sharp than those for 700#2 and 650#1. This indicates that the orthorhombic crystals in 800#1 and 700#1 are less ordered than those in 700#2 and 650#1. It is expected that 700#1 and 700#2 have the same crystal orderliness because they were prepared under the same experimental condition. The difference between these two might indicate low reproducibility of the annealing at 700°C, possibly because this temperature is close to the orthorhombic-to-tetragonal transition temperature, as will be discussed in the next paragraph.

Figure 8 shows the *a* and *b* axes of $DyBa_2Cu_3O_{7-\delta}$ as a function of the annealing temperature. Around 700°C, the orthorhombic *a* and *b* axes merge into the corresponding tetragonal axes, suggesting that the temperature between 650 and 700°C is approximately the orthorhombic-to-tetragonal transition temperature. This coincides with the previous observation. According to Bukanko et al.[14], the δ value at the orthorhombic-to-tetragonal transition is about 0.64. Therefore, we conclude that the samples prepared at around 650 and 700°C have a δ value of ca. 0.64.

Conclusions

A mixture of two crystal forms (orthorhombic and tetragonal) of $DyBa_2Cu_3O_{7-\delta}$ was studied using the XRD method. The two crystal forms were clearly identified using the 2D XRD profiles obtained by in situ XRD measurements with and without sample rotation under the magnetic field. When it is difficult to distinguish the crystal forms using the powder method alone because the lattice parameters are very close, the 2D XRD technique used in this work is very useful for easily and accurately distinguishing the two crystal forms.

Author Contributions

The manuscript was written through contributions of all authors. All authors have given approval to the final version of the manuscript. These authors contributed equally.

Conflicts of interest

There are no conflicts to declare.

Acknowledgements

This work was partly supported by the Adaptable and Seamless Technology Transfer Program through Target-Driven R&D (A-STEP), the Japan Science and Technology Agency (JST) and JSPS KAKENHI Grant Number JP17H03235.

References

1 T. W. Clinton, J. W. Lynn, J. Z. Liu, Y. X. Jia, T. J. Goodwin, R. N. Shelton, B. W. Lee, M. Buchgeister, M. B. Maple, and J. L. Peng, *Phys Rev B Condens Matter*, 1995, **51**, 15429.
2 R. H. Hammond and R. Bormann, *Physica C*, 1989, **162-164**, 703.
3 R. J. Cava, A. W. Hewat, E. A. Hewat, B. Batlogg, M. Marezio, K. M. Rabe, J. J. Krajewski, W. F. Peck Jr., *Physica C*, 1990, **165**, 419.
4 M. Yamaki, S. Horii, M. Haruta, J.-i. Shimoyama, *Jpn. J. Appl. Phys.*, 2012, **51**, 010107.
5 S. Horii, S. Okuhira, M. Yamaki, K. Kishio, J.-i. Shimoyama, T. Doi, *J. Appl. Phys.*, 2014, **115**, 113908.
6 K. Matsumoto, F. Kimura, G. Song, S. Yamane, H. Kikuchi, T. Tanaka, S. Higuchi, N. Kitamura, T. Kimura, *Crystal Growth & Design*, 2014, **14**, 6486.
7 H. Miura, *Journal of the Crystallographic Society of Japan*, 2003, **45**, 145.
8 M. Muralidhary, H. S. Chauhany, T. Saitohz, K. Kamadaz, K. Segawaz, and M. Murakamiy, *Superconductor Science and Technology*, 1997, **10**, 663.
9 F. Kimura, T. Kimura, *CrystEngComm*, 2018, **20**, 861.
10 ICDD, PDF card number: 1538675.
11 A. Ishihara, S. Horii, T. Uchikoshi, T. S. Suzuki, Y. Sakka, H. Ogino, J.-i. Shimoyama, and K. Kishio, *Applied Physics Express 2008*, **1**, 031701.
12 S. Adachi, A. Ichinose, F. Kimura, and S. Horii, *IEEE Transactions on Applied Superconductivity*, 2022, **2**, 1.
13 S. Horii, S. Fujioka, and T. Doi, *Jpn. J. Appl. Phys.*, 2018, **57**, 093101.
14 F. N. Bukhanko, N. A. Doroshenko, and V. I. Kamenev, *Journal of Magnetism and Magnetic Materials*, 2002, **242-245**, 1100.

